IEEE Access
Multidisciplinary | Rapid Review | Open Access Journal

Received May 18, 2019, accepted June 10, 2019, date of publication June 19, 2019, date of current version July 16, 2019.

Digital Object Identifier 10.1109/ACCESS.2019.2923650

On the Volume-Surface Integral Equation for Scattering From Arbitrary Shaped Composite PEC and Inhomogeneous Bi-Isotropic Objects

JINBO LIU[1], ZENGRUI LI[1], (Member, IEEE), JIANXUN SU[1], AND JIMING SONG[2], (Fellow, IEEE)

[1]School of Information and Communication Engineering, Communication University of China, Beijing 100024, China
[2]Department of Electrical and Computer Engineering, Iowa State University, Ames, IA 50011, USA

Corresponding author: Zengrui Li (zrli@cuc.edu.cn)

This work was supported in part by the National Natural Science Foundation of China under Grant 61701447, Grant 61671415, and Grant 61331002, and in part by the Fundamental Research Funds for the Central Universities under Grant CUC2019B068 and Grant CUC18A007.

ABSTRACT A new generalized volume-surface integral equation, volume integral equation-combined field integral equation (VIE-CFIE), is proposed to analyze the electromagnetic (EM) scattering from composite objects comprised of both perfect electric conductor (PEC) and inhomogeneous bi-isotropic material. By discretizing the objects using triangular and tetrahedral cells on which the commonly used Rao-Wilton-Glisson (RWG) and Schaubert-Wilton-Glisson (SWG) basis functions are respectively defined, the matrix equation is derived using the method of moments (MoM) and the Galerkin's testing. Furthermore, the continuity condition (CC) of electric flux is explicitly enforced on the PEC and bi-isotropy interfaces. In this way, the number of volumetric unknowns is reduced based on the same set of meshes, particularly for the thin coated PEC objects. A convenient way to embed the CC into the context of MoM solution is provided in detail. Several numerical results of EM scattering from coated PEC objects are shown to illustrate the accuracy and efficiency of the proposed method.

INDEX TERMS Bi-isotropy, continuity condition (CC), integral equations, method of moments (MoM).

I. INTRODUCTION

With the rapid development of material science, quantities of researches focus on the bi-isotropic materials since their applications are various, such as in antenna design [1], waveguide mode converters [2], radar absorbers, electromagnetic (EM) stealth [3], [4], and many other microwave and millimeter-wave devices [5], [6]. Consequently, the EM radiation or scattering properties of composite objects containing perfect electric conductors (PECs) and bi-isotropic materials have aroused great interests in the field of computational electromagnetics. However, because the constitutive relations of bi-isotropy are enforced an additional coupling between the electric and magnetic fields, it is quite a challenge to accurately analyze such composite objects. Some articles have discussed the power of full-wave methods [7]–[11]. In [7], the finite-difference time-domain method was presented to solve the bi-isotropic coated PEC bodies. However, when the shape of the analyzed object is arbitrary, the reliability of this method still needs to be further investigated. In [8], EM scattering from chiral objects above a perfectly electric or magnetic conducting plane was analyzed by the hybrid finite element-boundary integral method. EM scattering by arbitrarily shaped PEC objects coated with homogenous bi-isotropic materials was calculated by using the surface integral equation (SIE) method [9]. Later, a volume integral equation (VIE) was formulated for objects with inhomogeneous bi-isotropy [10]. Nevertheless, the PECs cannot be modeled directly, which need to be replaced by lossy dielectric with sufficient high conductivity. In [11], the multilevel Green's function interpolation method is developed to analyze the EM scattering from objects comprised of both PEC and bi-isotropic material. However, due to the use of hexahedral meshes, whether it is suitable for objects containing sharp

The associate editor coordinating the review of this manuscript and approving it for publication was Muhammad Zubair.

structures needs further verification. Some novel methods for the simulation of composite objects are shown in [12]–[14].

Among numerous numerical methods, the method of moments (MoM) solution of volume-surface integral equation (VSIE) is one of top choices to analyze the general composite PEC-material objects [15], [16]. Compared to the pure SIE-based methods such as the so-called PMCHWT or the Müller formulations, the VSIE is more robust and generalized in modeling composite objects containing thin inhomogeneous materials with corners and edges [17]. This generality owes to the fact that according to the equivalence principle, the VSIE implementation simultaneously retains two generally applicable integral equations: the VIE to model the field superposition in the material regions, and the SIE to enforce the boundary conditions on the PEC surfaces. For the SIE part of VSIE, the electric field integral equation (EFIE) is commonly adopted since it can be used to model both the open and the closed PEC surfaces. However, the EFIE is a first-kind integral equation, usually resulting in an ill-conditioned matrix generated by the whole VSIE. To improve the condition, when modeling the closed PEC surfaces, the magnetic field integral equation (MFIE) can be linearly added to the EFIE to form the well-conditioned combined field integral equation (CFIE) which is the second-kind. Furthermore, the CFIE can be combined with the VIE to yield a new generalized VSIE form, called VIE-CFIE, which is expected to make the matrix equation more easily to solve than the conventional VIE-EFIE form. In addition, lots of the composite objects are composed of PECs and materials in contact. For these objects, the continuity condition (CC) of electric flux can be explicitly enforced on the PEC-material interfaces to eliminate the associated volumetric unknowns. In [16], [18] and [19], how the CC is adopted in the VSIE was discussed. However, the validity was not studied rigorously. In [20], for the higher-order Legendre basis functions with the property of orthogonality, the CC can be explicitly enforced on any PEC-electrical isotropy interfaces. Nevertheless, when the lower-order basis functions are adopted, whether the use of CC is still valid was not considered. The validity of the use of CC was investigated in [21]. It is stated that if the involved PEC surfaces are open, the induced surface electric current is actually the summation of current densities residing on both sides [22]. In this case, the explicit enforcement of CC in the VSIE might lead to inaccurate results.

To the authors' best knowledge, so far the VIE-CFIE and the CC only have been applied to the composite PEC-electrical isotropy objects, while no literature devotes to discussing such implementations to other kinds of materials. In this paper, the VIE-CFIE is extended to analyze the EM scattering from composite objects comprised of both closed PECs and inhomogeneous bi-isotropic materials. By discretizing the equivalent currents using the commonly used Rao-Wilton-Glisson (RWG) [23] and Schaubert-Wilton-Glisson (SWG) [24] basis functions defined on the triangular and tetrahedral cells, and combining with the Galerkin's method, the VIE-CFIE yields a well-conditioned matrix equation. The calculation of matrix elements is discussed in detail. Furthermore, during the solving of the presented VIE-CFIE, in order to reduce the volumetric unknowns and the memory requirement without compromising the numerical accuracy, how to enforce the CC to the arbitrary PEC-bi-isotropy interfaces is shown. A convenient way to embed the CC into the context of the MoM solution is also provided.

II. THEORY AND FORMULATIONS

A. DERIVATION OF VSIE FOR COMPOSITE PEC-BI-ISOTROPIC OBJECTS

Consider an arbitrary PEC surface S, partly or wholly covered by inhomogeneous bi-isotropic material occupying a region V. For the convenience of analysis, assume that this composite object is suspended in free space, and illuminated by an incident EM plane wave $(\vec{E}^i, \vec{H}^i)$ at an arbitrary angle to radiate the scattered field $(\vec{E}^s, \vec{H}^s)$. Thus, the total EM field $(\vec{E}, \vec{H})$ is the summation of incident and scattered fields as

$$\left(\vec{E}, \vec{H}\right) = \left(\vec{E}^i, \vec{H}^i\right) + \left(\vec{E}^s, \vec{H}^s\right) \tag{1}$$

In the inhomogeneous bi-isotropic region V, the coupled constitutive relations between the electric flux density $\vec{D}$, magnetic flux density $\vec{B}$ and the electric field $\vec{E}$, magnetic field $\vec{H}$ are written as

$$\begin{bmatrix} \vec{D}(\vec{r}) \\ \vec{B}(\vec{r}) \end{bmatrix} = \begin{bmatrix} \varepsilon(\vec{r}) & \xi(\vec{r}) \\ \varsigma(\vec{r}) & \mu(\vec{r}) \end{bmatrix} \begin{bmatrix} \vec{E}(\vec{r}) \\ \vec{H}(\vec{r}) \end{bmatrix} \quad \forall \vec{r} \in V \tag{2}$$

where all of the medium parameters, i.e. permittivity ε, permeability μ, and bi-isotropic parameters ξ, ς, are $\vec{r}$-dependent. For easy reading, the variable $\vec{r}$ will be omitted from the following equations. (2) can also be rewritten as

$$\begin{bmatrix} \vec{E} \\ \vec{H} \end{bmatrix} = \frac{1}{\varepsilon\mu - \xi\zeta} \begin{bmatrix} \mu & -\xi \\ -\varsigma & \varepsilon \end{bmatrix} \begin{bmatrix} \vec{D} \\ \vec{B} \end{bmatrix} = \begin{bmatrix} \alpha_{11} & \alpha_{12} \\ \alpha_{21} & \alpha_{22} \end{bmatrix} \begin{bmatrix} \vec{D} \\ \vec{B} \end{bmatrix} \tag{3}$$

As we know, the EM field in the source-free domain conforms to the Maxwell's equations, which is independent of the type of media. Thus, we can rearrange the two well-known curl equations for the total EM field $(\vec{E}, \vec{H})$ by substituting with (2) as

$$\begin{cases} \nabla \times \vec{E} = -j\omega\vec{B} = -j\omega\left(\varsigma\vec{E} + \mu\vec{H}\right) \\ \nabla \times \vec{H} = j\omega\vec{D} = j\omega\left(\varepsilon\vec{E} + \xi\vec{H}\right) \end{cases} \tag{4}$$

with the angular frequency ω and $j = \sqrt{-1}$, while the time-harmonic factor is $e^{j\omega t}$. In a similar way, the incident wave $(\vec{E}^i, \vec{H}^i)$ in a source-free free space satisfies

$$\begin{cases} \nabla \times \vec{E}^i = -j\omega\mu_0\vec{H}^i \\ \nabla \times \vec{H}^i = j\omega\varepsilon_0\vec{E}^i \end{cases} \tag{5}$$

where ε_0 and μ_0 are the permittivity and permeability of the free space, respectively. By subtracting (5) from (4), it is obtained

$$\begin{cases} \nabla \times \vec{E}^s = -j\omega\mu_0\vec{H}^s - j\omega(\mu - \mu_0)\vec{H} - j\omega\varsigma\vec{E} \\ \nabla \times \vec{H}^s = j\omega\varepsilon_0\vec{E}^s + j\omega(\varepsilon - \varepsilon_0)\vec{E} + j\omega\xi\vec{H} \end{cases} \tag{6}$$

According to the volume equivalence principle, the scattered field from the bi-isotropy can be seen as producing by both the equivalent volume electric and magnetic currents, $\vec{J}_V$ and $\vec{M}_V$, in the free space. By comparing (6) with the two curl Maxwell's equations, $\vec{J}_V$ and $\vec{M}_V$ for bi-isotropic materials are derived by

$$\begin{bmatrix} \vec{J}_V \\ \vec{M}_V \end{bmatrix} = j\omega \begin{bmatrix} \varepsilon - \varepsilon_0 & \xi \\ \varsigma & \mu - \mu_0 \end{bmatrix} \begin{bmatrix} \vec{E} \\ \vec{H} \end{bmatrix} \tag{7}$$

Substituting (3) into (7) yields

$$\begin{aligned} \begin{bmatrix} \vec{J}_V \\ \vec{M}_V \end{bmatrix} &= j\omega \begin{bmatrix} 1 - \varepsilon_0\alpha_{11} & -\varepsilon_0\alpha_{12} \\ -\mu_0\alpha_{21} & 1 - \mu_0\alpha_{22} \end{bmatrix} \begin{bmatrix} \vec{D} \\ \vec{B} \end{bmatrix} \\ &= j\omega \begin{bmatrix} \beta_{11} & \beta_{12} \\ \beta_{21} & \beta_{22} \end{bmatrix} \begin{bmatrix} \vec{D} \\ \vec{B} \end{bmatrix} \end{aligned} \tag{8}$$

The scattered field is cast in terms of mixed auxiliary potentials due to $\vec{J}_V$, $\vec{M}_V$ and the induced surface electric current $\vec{J}_S$ on the PEC surface S as

$$\begin{cases} \vec{E}^s = -j\omega\left(\vec{A}_S^J + \vec{A}_V^J\right) - \nabla\left(\varphi_S^J + \varphi_V^J\right) - \dfrac{1}{\varepsilon_0}\nabla \times \vec{A}_V^M \\ \vec{H}^s = \dfrac{1}{\mu_0}\nabla \times \left(\vec{A}_S^J + \vec{A}_V^J\right) - j\omega\vec{A}_V^M - \nabla\varphi_V^M \end{cases} \tag{9}$$

respectively, while the vector and the scalar potentials are expressed as the convolutions of equivalent currents or their divergences and the Green's function as

$$\begin{cases} \vec{A}_T^J(\vec{r}) = \mu_0 \displaystyle\int_T \vec{J}_T(\vec{r}')\, G(\vec{r}, \vec{r}')\, dT' \\ \varphi_T^J(\vec{r}) = \dfrac{j}{\omega\varepsilon_0} \displaystyle\int_T \nabla' \cdot \vec{J}_T(\vec{r}')\, G(\vec{r}, \vec{r}')\, dT' \end{cases} \tag{10}$$

where $T = S$ or V for surface or volume integrals over the surface or volume currents, respectively. $\vec{A}_V^M$, φ_V^M can be found using the duality. Besides, the Green's function of free space is expressed as

$$G\left(\vec{r}, \vec{r'}\right) = \frac{e^{-jk_0|\vec{r}-\vec{r}'|}}{4\pi\,|\vec{r}-\vec{r}'|} \tag{11}$$

with the wavenumber $k_0 = \omega\sqrt{\mu_0\varepsilon_0}$.

In the region V, the VIE is formed by making the total field equal to the sum of the incident and the scattered fields as

$$\begin{aligned} &\left[\vec{E}(\vec{r}), \vec{H}(\vec{r})\right] - \left[\vec{E}^s(\vec{r}), \vec{H}^s(\vec{r})\right] \\ &\quad = \left[\vec{E}^i(\vec{r}), \vec{H}^i(\vec{r})\right] \end{aligned} \quad \forall \vec{r} \in V \tag{12}$$

On the PEC surface S, the EFIE is formed based on the PEC boundary condition that requires vanishing the tangential component of total electric field as

$$\hat{n}(\vec{r}) \times \vec{E}(\vec{r}) = \hat{n}(\vec{r}) \times \left[\vec{E}^i(\vec{r}) + \vec{E}^s(\vec{r})\right] = 0 \quad \forall \vec{r} \in S \tag{13}$$

The EFIE is combined with the VIE to form the commonly used EFIE-VIE, a first-kind form of VSIE that is ill-conditioned at the resonant frequencies. Furthermore, for the closed PEC surface, the MFIE

$$\frac{1}{2}\vec{J}_S(\vec{r}) - \hat{n}(\vec{r}) \times \vec{H}^s(\vec{r}) = \hat{n}(\vec{r}) \times \vec{H}^i(\vec{r}) \quad \forall \vec{r} \in S \tag{14}$$

can be linearly added to the EFIE to form the well-conditioned CFIE as

$$CFIE = \alpha EFIE + (1 - \alpha)\,\eta_0 MFIE \tag{15}$$

where α ($0 \le \alpha \le 1$) is a real constant, and η_0 is the intrinsic impedance of free space. We can combine the VIE in (12) and the CFIE in (15) together to build the well-conditioned VIE-CFIE, a second-kind VSIE form, to solve the EM scattering from composite objects involving open or closed PEC surfaces and bi-isotropic materials. In this paper, for the closed PEC surfaces, $\alpha = 0.5$, while for the open, α must be fixed to 1.

Furthermore, on the PEC-bi-isotropy interfaces S', the CC establishes the relation between $\vec{D}$ and $\vec{J}_S$, which can be written as

$$\hat{n}(\vec{r}) \cdot \vec{D}(\vec{r}) = \rho_S(\vec{r}) = -\frac{\nabla \cdot \vec{J}_S(\vec{r})}{j\omega} \quad \forall \vec{r} \in S' \tag{16}$$

with the electric charge density ρ_S on the PEC surface. Since the CC conforms to the current continuity equation that is independent of the type of media, it can be safely adopted to the PEC-bi-isotropy interfaces.

B. MOM SOLUTION USING GALERKIN'S TESTING

Using the MoM, the VSIE is discretized into a matrix equation. In the implementation, the RWG basis functions $\vec{f}_i^S$ [23] and SWG basis functions $\vec{f}_i^V$ [24] are used to expand $\vec{J}_S$ on S and $\vec{D}$ and $\vec{B}$ in V as

$$\begin{cases} \vec{J}_S = \displaystyle\sum_{i=1}^{N_S} I_i^S \vec{f}_i^S \\ j\omega\vec{D} = \displaystyle\sum_{i=1}^{N_V} I_i^D \vec{f}_i^V \\ \dfrac{j\omega}{\eta_0}\vec{B} = \displaystyle\sum_{i=1}^{N_V} I_i^B \vec{f}_i^V \end{cases} \tag{17}$$

respectively. In (17), N_S and N_V are the numbers of RWG and SWG basis functions, while the total number of unknowns is $N_S + 2N_V$. I_i^S, I_i^D and I_i^B are the corresponding unknown expansion coefficients, respectively. Dispersing $\vec{D}$ and $\vec{B}$ instead of $\vec{J}_V$ and $\vec{M}_V$ can hold the continuity of the normal component that is consistent with the boundary condition for material interfaces. It is worthy to mention that at the exterior boundary of materials, since $\vec{D}$ and $\vec{B}$ are not necessarily zero, "half" SWG basis functions associated with only one tetrahedron need to be defined [24]. It is further assumed that parameters ε, μ, ξ and ς are approximately constant within each tetrahedron, which is a generalization of that presented in [24]. As a consequence, the 2×2 matrices $[\alpha]$ and $[\beta]$ defined in (3) and (8) over a single tetrahedron are also considered as approximately matrices, the elements of which will be denoted by α_{ipq} and β_{ipq} with $p/q = 1, 2$ in the following, respectively.

Substituting (17) into (7), we obtain

$$\begin{cases} \vec{J}_V = \sum_{i=1}^{N_V} I_i^D \left(\beta_{i11}\vec{f}_i^V\right) + \sum_{i=1}^{N_V} I_i^B \left(\beta_{i12}\vec{f}_i^V\right) \\ \vec{M}_V = \sum_{i=1}^{N_V} I_i^D \left(\beta_{i21}\vec{f}_i^V\right) + \sum_{i=1}^{N_V} I_i^B \left(\beta_{i22}\vec{f}_i^V\right) \end{cases} \tag{18}$$

Substituting (18) into (9)-(15) and combining with Galerkin's testing result in an impedance matrix equation, which can succinctly be represented as

$$\begin{bmatrix} Z_{SS} & Z_{SD} & Z_{SB} \\ Z_{DS} & Z_{DD} & Z_{DB} \\ Z_{BS} & Z_{BD} & Z_{BB} \end{bmatrix} \begin{Bmatrix} I_S \\ I_D \\ I_B \end{Bmatrix} = \begin{Bmatrix} V_S \\ V_D \\ V_B \end{Bmatrix} \tag{19}$$

with

$$\begin{aligned} [Z_{SS}] &= \alpha \left[Z_{SS}^E\right] + (1-\alpha)\,\eta_0 \left[Z_{SS}^M\right] \\ [Z_{SD}] &= \alpha \left[Z_{SD}^E\right] + (1-\alpha)\,\eta_0 \left[Z_{SD}^M\right] \\ [Z_{SB}] &= \alpha \left[Z_{SB}^E\right] + (1-\alpha)\,\eta_0 \left[Z_{SB}^M\right] \\ \{V_S\} &= \alpha \left\{V_S^E\right\} + (1-\alpha)\,\eta_0 \left\{V_S^M\right\} \end{aligned} \tag{20}$$

where $\{I_S\}$, $\{I_D\}$ and $\{I_B\}$ are the vectors of unknown expansion coefficients, $\{V_S\}$, $\{V_D\}$ and $\{V_B\}$ are the excitation vectors, respectively. $[Z_{PQ}]$ ($P/Q = S$, D, or B) denotes the impedance sub-matrix representing the interactions between various types of testing and basis functions defined above. For convenience, three linear vector operators are defined as

$$\begin{cases} \vec{P}_{T_i}\left(\vec{X}\right) = \int_{T_i} \vec{X}\left(\vec{r}'\right) G\left(\vec{r},\vec{r}'\right) dT' \\ \vec{Q}_{T_i}\left(\vec{X}\right) = \nabla \int_{T_i} \nabla' \cdot \vec{X}\left(\vec{r}'\right) G\left(\vec{r},\vec{r}'\right) dT' \qquad T = S \text{ or } V \\ \vec{K}_{T_i}\left(\vec{X}\right) = \int_{T_i} \vec{X}\left(\vec{r}'\right) \times \nabla G\left(\vec{r},\vec{r}'\right) dT' \end{cases} \tag{21}$$

Fully taking the advantage of the symmetry of matrix entries to simplify the matrix filling process, each submatrix entry in jth row, ith column is then given by

$$\begin{aligned} \left[Z_{SS}^E\right]_{ji} &= j\omega\mu_0 \left\langle \vec{f}_j^S(\vec{r}), \vec{P}_{S_i}\left(\vec{f}_i^S\right)\right\rangle \\ &\quad + \frac{j}{\omega\varepsilon_0} \left\langle \vec{f}_j^S(\vec{r}), \vec{Q}_{S_i}\left(\vec{f}_i^S\right)\right\rangle \end{aligned} \tag{22}$$

$$\left[Z_{SS}^M\right]_{ji} = \frac{1}{2}\left\langle \vec{f}_j^S(\vec{r}), \vec{f}_i^S(\vec{r})\right\rangle + \left\langle \vec{f}_j^S(\vec{r}) \times \hat{n}(\vec{r}), \vec{K}_{S_i}\left(\vec{f}_i^S\right)\right\rangle \tag{23}$$

$$\begin{aligned} [Z_{DS}]_{ji} &= j\omega\mu_0 \left\langle \vec{f}_j^V(\vec{r}), \vec{P}_{S_i}\left(\vec{f}_i^S\right)\right\rangle \\ &\quad + \frac{j}{\omega\varepsilon_0} \left\langle \vec{f}_j^V(\vec{r}), \vec{Q}_{S_i}\left(\vec{f}_i^S\right)\right\rangle \end{aligned} \tag{24}$$

$$[Z_{BS}]_{ji} = \left\langle \vec{f}_j^V(\vec{r}), \vec{K}_{S_i}\left(\vec{f}_i^S\right)\right\rangle \tag{25}$$

and

$$\begin{cases} \left[Z_{SD}^E\right]_{ji} = Z_{ji}^E(\beta_{i11}, \beta_{i21}) \\ \left[Z_{SB}^E\right]_{ji} = Z_{ji}^E(\beta_{i12}, \beta_{i22}) \\ \left[Z_{SD}^M\right]_{ji} = Z_{ji}^M(\beta_{i11}, \beta_{i21}) \\ \left[Z_{SB}^M\right]_{ji} = Z_{ji}^M(\beta_{i12}, \beta_{i22}) \\ [Z_{DD}]_{ji} = Z_{ji}^V(\alpha_{i11}, \beta_{i11}, \beta_{i21}, \varepsilon_0, \mu_0) \\ [Z_{DB}]_{ji} = Z_{ji}^V(\alpha_{i12}, \beta_{i12}, \beta_{i22}, \varepsilon_0, \mu_0) \\ [Z_{BD}]_{ji} = Z_{ji}^V(\alpha_{i21}, \beta_{i21}, -\beta_{i11}, \mu_0, \varepsilon_0) \\ [Z_{BB}]_{ji} = Z_{ji}^V(\alpha_{i22}, \beta_{i22}, -\beta_{i12}, \mu_0, \varepsilon_0) \end{cases} \tag{26}$$

where

$$\begin{aligned} Z_{ji}^E(\beta_{ip_1q}, \beta_{ip_2q}) &= j\omega\mu_0\beta_{ip_1q} \left\langle \vec{f}_j^S(\vec{r}), \vec{P}_{V_i}\left(\vec{f}_i^V\right)\right\rangle \\ &\quad + \frac{j}{\omega\varepsilon_0}\beta_{ip_1q} \left\langle \vec{f}_j^S(\vec{r}), \vec{Q}_{V_i}\left(\vec{f}_i^V\right)\right\rangle \\ &\quad - \beta_{ip_2q} \left\langle \vec{f}_j^S(\vec{r}), \vec{K}_{V_i}\left(\vec{f}_i^V\right)\right\rangle \end{aligned} \tag{27}$$

$$\begin{aligned} Z_{ji}^M(\beta_{ip_1q}, \beta_{ip_2q}) &= \beta_{ip_1q} \left\langle \vec{f}_j^S(\vec{r}) \times \hat{n}(\vec{r}), \vec{K}_{V_i}\left(\vec{f}_i^V\right)\right\rangle \\ &\quad + j\omega\varepsilon_0\beta_{ip_2q} \left\langle \vec{f}_j^S(\vec{r}) \times \hat{n}(\vec{r}), \vec{P}_{V_i}\left(\vec{f}_i^V\right)\right\rangle \\ &\quad + \frac{j}{\omega\mu_0}\beta_{ip_2q} \left\langle \vec{f}_j^S(\vec{r}) \times \hat{n}(\vec{r}), \vec{Q}_{V_i}\left(\vec{f}_i^V\right)\right\rangle \end{aligned} \tag{28}$$

$$\begin{aligned} &Z_{ji}^V(\alpha_{ip_1q}, \beta_{ip_1q}, \beta_{ip_2q}, \chi, \gamma) \\ &= \frac{1}{j\omega}\alpha_{ip_1q} \left\langle \vec{f}_j^V(\vec{r}), \vec{f}_i^V(\vec{r})\right\rangle \\ &\quad + j\omega\gamma\beta_{ip_1q} \left\langle \vec{f}_j^V(\vec{r}), \vec{P}_{V_i}\left(\vec{f}_i^V\right)\right\rangle \\ &\quad + \frac{j}{\omega\chi}\beta_{ip_1q} \left\langle \vec{f}_j^V(\vec{r}), \vec{Q}_{V_i}\left(\vec{f}_i^V\right)\right\rangle \\ &\quad - \beta_{ip_2q} \left\langle \vec{f}_j^V(\vec{r}), \vec{K}_{V_i}\left(\vec{f}_i^V\right)\right\rangle \end{aligned} \tag{29}$$

where $p_1/p_2/q = 1$ or 2 and $p_1 + p_2 \equiv 3$. The details of the calculation of matrix entries are described in the Appendixes.

C. APPLYING THE CONTINUITY CONDITION

Consider a composite object containing any arbitrary PEC-bi-isotropic material contact. As shown in Fig. 1, after discretization, assume a tetrahedron with one face exactly overlapped by the kth PEC triangular cell. In this tetrahedron, the pth "half" SWG basis function is defined over the PEC face with the expansion coefficient of $\vec{D}$ being I_p^D. Besides, assume that the indices of the three associated RWG functions defined on the corresponding PEC triangle are k_1, k_2, and k_3 with the corresponding coefficients $I_{k_1}^S$, $I_{k_2}^S$, and $I_{k_3}^S$, respectively. In the traditional MoM, I_p^D is considered independent of $I_{k_1}^S$, $I_{k_2}^S$, and $I_{k_3}^S$. Actually, according to the CC, these coefficients are related however. According to (16)

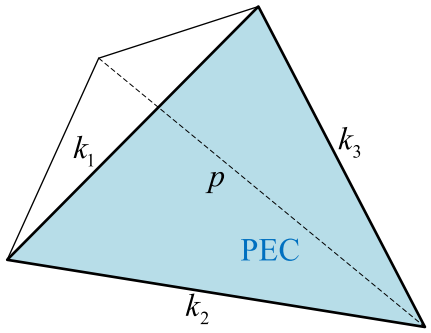

FIGURE 1. RWG and SWG basis functions on the PEC-material interface.

and (17), I_p^D can be directly calculated by

$$I_p^D = -\frac{\sum_{i=1}^{3} I_{k_i}^S \nabla \cdot \vec{f}_{k_i}^S(\vec{r})}{\hat{n}(\vec{r}) \cdot \vec{f}_p^V(\vec{r})} = -\mathrm{sgn}(p) \sum_{i=1}^{3} I_{k_i}^S \mathrm{sgn}(k_i) \frac{l_{k_i}}{A_k} \quad (30)$$

where $\mathrm{sgn}(k_i) = 1$ or -1 means that the current direction of the k_ith basis function is outward or inward relative to the kth triangle, and $\mathrm{sgn}(p)$ is the pth "half" SWG function relative to the tetrahedron, respectively. l_{k_i} is the length of the k_ith edge, and A_k is the area of the kth triangle. That is to say, when the CC is enforced, the volumetric unknown expansion coefficients of $\vec{D}$ associated to the PEC-bi-isotropy interfaces can be directly calculated by the surface unknown expansion coefficients of $\vec{J}_S$ defined on the overlapped PEC surface, instead of independently solving them from the matrix equation.

The following will show how to merge the CC into the matrix equation during the iterative solving. We further classify $\{I_D\}$ into two groups: $\{I_{D_2}\}$ is the unknown vector related to the "half" SWG basis functions defined on the tetrahedrons with one or more faces terminated by PEC surfaces, while $\{I_{D_1}\}$ is the vector of the other SWG functions. The numbers of elements of $\{I_{D_1}\}$ and $\{I_{D_2}\}$ are N_{V_1} and N_{V_2}, respectively, while $N_{V_1}+N_{V_2} = N_V$. Similarly, $\{I_S\}$ is also classified into two groups: $\{I_{S_2}\}$ is the unknown vector of the RWG functions defined on the PEC triangular faces overlapping the tetrahedrons, while $\{I_{S_1}\}$ is the vector of the other RWG functions. The numbers of elements of $\{I_{S_1}\}$ and $\{I_{S_2}\}$ are N_{S_1} and N_{S_2} with $N_{S_1}+N_{S_2} = N_S$, respectively. Thus, the matrix equation shown in (19) can be divided into

$$\begin{bmatrix} Z_{S_1S_1} & Z_{S_1S_2} & Z_{S_1D_1} & Z_{S_1D_2} & Z_{S_1B} \\ Z_{S_2S_1} & Z_{S_2S_2} & Z_{S_2D_1} & Z_{S_2D_2} & Z_{S_2B} \\ Z_{D_1S_1} & Z_{D_1S_2} & Z_{D_1D_1} & Z_{D_1D_2} & Z_{D_1B} \\ Z_{D_2S_1} & Z_{D_2S_2} & Z_{D_2D_1} & Z_{D_2D_2} & Z_{D_2B} \\ Z_{BS_1} & Z_{BS_2} & Z_{BD_1} & Z_{BD_2} & Z_{BB} \end{bmatrix} \begin{Bmatrix} I_{S_1} \\ I_{S_2} \\ I_{D_1} \\ I_{D_2} \\ I_B \end{Bmatrix} = \begin{Bmatrix} V_{S_1} \\ V_{S_2} \\ V_{D_1} \\ V_{D_2} \\ V_B \end{Bmatrix} \quad (31)$$

Besides, relating the expansion coefficients, (30) can be rewritten as the following matrix equation

$$\{I_{D_2}\} = [\bar{D}]\{I_{S_2}\} \quad (32)$$

where $[\bar{D}]$ is a sparse matrix of size $N_{V_2} \times N_{S_2}$, and each row has only three nonzero elements as

$$[\bar{D}]_{pk_i} = -\mathrm{sgn}(p)\,\mathrm{sgn}(k_i)\frac{l_{k_i}}{A_k} \quad i = 1, 2, 3 \quad (33)$$

Substituting (32) into (31) yields

$$\begin{bmatrix} Z_{S_1S_1} & Z_{S_1S_2}+Z_{S_1D_2}\bar{D} & Z_{S_1D_1} & Z_{S_1B} \\ Z_{S_2S_1} & Z_{S_2S_2}+Z_{S_2D_2}\bar{D} & Z_{S_2D_1} & Z_{S_2B} \\ Z_{D_1S_1} & Z_{D_1S_2}+Z_{D_1D_2}\bar{D} & Z_{D_1D_1} & Z_{D_1B} \\ Z_{BS_1} & Z_{BS_2}+Z_{BD_2}\bar{D} & Z_{BD_1} & Z_{BB} \end{bmatrix} \begin{Bmatrix} I_{S_1} \\ I_{S_2} \\ I_{D_1} \\ I_B \end{Bmatrix} = \begin{Bmatrix} V_{S_1} \\ V_{S_2} \\ V_{D_1} \\ V_B \end{Bmatrix} \quad (34)$$

It can be seen that the unknown vector $\{I_{D_2}\}$ is eliminated. Compared (34) to (31), the size of the matrix is reduced from $(N_S+2N_V)\times(N_S+2N_V)$ to $(N_S+N_{V_1}+N_V)\times(N_S+N_{V_1}+N_V)$. Therefore, if N_{V_2} is relatively large with respect to the total number of unknowns N, the matrix filling time, the peak memory requirement, and the matrix-vector product time will be decreased significantly. Furthermore, since the use of CC leads to less number of unknown coefficients, the total iteration numbers are also expected less than the one without the CC.

III. NUMERICAL RESULTS

In this section, the bistatic or monostatic radar cross section (RCS) results of several PEC objects coated with bi-isotropic material are calculated. Restarted GMRES with a restart parameter m is used as the iterative solver to reach convergence with relative residual error of 0.001, while m is fixed to 50 [25]. A simple diagonal preconditioner is used to accelerate the iterative solving process. A zero vector is taken as initial guess for all calculations. All computations are serially carried out on a workstation with 2.4 GHz CPU and 384 GB RAM in single precision.

In general, the Gaussian quadrature rule with 4/5 sampling points is applied to the inner or outer triangle/tetrahedron domain of integrations during calculating the interactions between the testing and basis functions [26], [27], which can ensure accurate calculation of up to 3rd order of polynomials. For the SIE part of the VSIE, the EFIE is known to give relatively accurate surface current $\vec{J}_S$ with the use of RWG basis function for the PEC surfaces with arbitrary planar triangulations. By contrast, the MFIE is inaccurate to some extent [28]. A probable reason is that in the MFIE, the two-dimensional mild logarithmic singularity of the outer field integration is usually overlooked with an insufficiently number of integration points inside the testing triangles. Therefore, since MFIE is involved in the VIE-CFIE, the obtained

TABLE 1. The maximal (MAX) and the Root-Mean-Square (RMS) errors of different implements compared with exact results in dB.

VSIE form	co-polarization		cross-polarization	
	MAX	RMS	MAX	RMS
VIE-EFIE	0.59	0.18	0.79	0.19
VIE-CFIE	0.74	0.20	0.85	0.21
CC-VIE-EFIE	0.83	0.22	0.89	0.21
CC-VIE-CFIE	0.91	0.23	0.84	0.22

$\vec{J}_S$ on the PEC surfaces may not be so accurate. When the CC is adopted, according to (32), inaccurate $\{I_{S_2}\}$ will directly lead to inaccurate $\{I_{D_2}\}$, which will further result in a less accurate result. Therefore, when the VIE-CFIE is applied, to relieve the slight error caused by the MFIE [28], 13 sampling points of up to 7$^{\text{th}}$ order of polynomials are used over the outer triangular integrations in the MFIE part [26].

The first object is a PEC sphere coated with homogeneous bi-isotropic material. The radius of the PEC sphere is $0.4\lambda_0$ (λ_0 is the wavelength in free space), and the thickness of coating material is $0.1\lambda_0$ with the medium parameters $\varepsilon = 2\varepsilon_0$, $\mu = \mu_0$, and $\xi = \zeta* = (0.5 - j0.5)\sqrt{\varepsilon_0\mu_0}$, while the superscript "$*$" denotes complex conjugate. After discretization with an average mesh size of $0.05\lambda_0$, the total number of triangles, tetrahedrons and unknowns are 1,378, 10,703 and 48,367 respectively, while $N_{V_2} = 1,378$, equaling to the number of PEC triangular cells. The coating material is modeled by two-layer tetrahedral meshes. This coated sphere is illuminated by a θ-polarized plane wave across $+z$-axis, and the observation range is $0 \leqslant \theta \leqslant 180°$ and $\varphi = 0$. During the calculation, both the VIE-EFIE and VIE-CFIE, and that enforced the CC (denoted by CC-VIE-EFIE and CC-VIE-CFIE), are used. The numerical results of bistatic RCS are shown in Fig. 2, while the exact results from Mie series are also given in this figure as references [10]. It is observed that for either the co- or cross-polarization, the numerical results from VIE-EFIE or VIE-CFIE with and without CC are almost in excellent agreement with the exact results everywhere. Table 1 lists the maximal (MAX) and the root-mean-square (RMS) errors of different implementations compared with the exact results, while the maximal errors occur over the valley range (in this case, about 100° for the co-polarization and 45° for the cross-polarization). Table 2 (CS1) lists the computational details of these four different types of implementations in terms of peak memory (*Mem*), filling time of matrix (T_f), time cost per iteration (T_m), and the number of iterations.

The second object is also a coated sphere. The radius of the PEC sphere is $0.5\lambda_0$, and the thickness of coating material is $0.05\lambda_0$. After discretization with an average mesh size of $0.05\lambda_0$, the total number of triangles, tetrahedrons and unknowns are 2,110, 7,057 and 36,055 with $N_{V_2} = 2,110$, respectively. In this case, the coating material is modeled by single layer tetrahedral meshes. The medium parameters are assumed to be functions of a variable ρ as well as (θ, φ)

TABLE 2. Computational details of the solving process for different implementations.

Object	VSIE form	*Mem* (GB)	T_f (min)	T_m (sec)	Iterations number
CS1 (coated sphere for ex1)	VIE-EFIE	17.7	80.3	4.19	176
	VIE-CFIE		87.8		41
	CC-VIE-EFIE	16.5	76.6	3.97	158
	CC-VIE-CFIE		83.1		38
CS2 (coated sphere for ex2)	VIE-EFIE	9.82	45.6	2.15	156
	VIE-CFIE		49.9		35
	CC-VIE-EFIE	8.73	42.2	1.91	150
	CC-VIE-CFIE		46.5		32
CA (coated almond)	VIE-EFIE	4.58	21.3	1.51	382
	VIE-CFIE		23.2		45
	CC-VIE-EFIE	4.09	20.1	1.36	351
	CC-VIE-CFIE		21.9		41

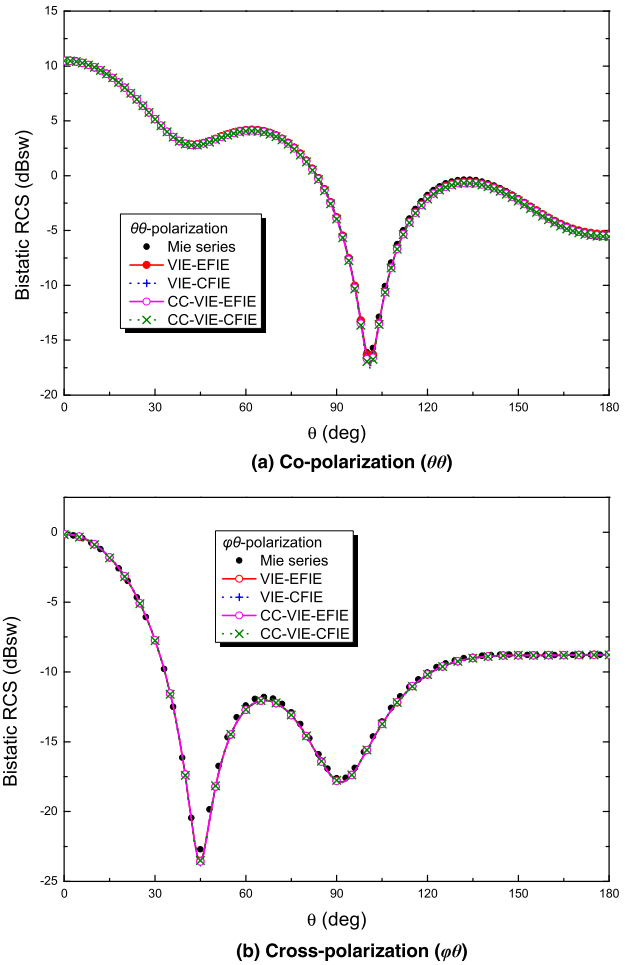

FIGURE 2. Bistatic RCS for a PEC sphere of radius $0.4\lambda_0$ coated with $0.1\lambda_0$ thick homogeneous bi-isotropic material with the medium parameters $\varepsilon = 2\varepsilon_0$, $\mu = \mu_0$, *and* $\xi = \zeta* = (0.5 - j0.5)\sqrt{\varepsilon_0\mu_0}$ at $0 \leq \theta \leq 180°$ and $\varphi = 0$, illuminated by a θ-polarized EM plane wave across $+z$ axis.

defined in the spherical coordinates as

$$\begin{cases} \varepsilon(\rho) = [1 + |\sin\theta\cos\varphi|\,\rho]\,\varepsilon_0 \\ \mu(\rho) = [1 + |\cos\theta\sin\varphi|\,\rho]\,\mu_0 \\ \xi(\rho) = \varsigma^*(\rho) = (0.1 - j0.1)\,\rho\sqrt{\varepsilon_0\mu_0} \end{cases} \tag{35}$$

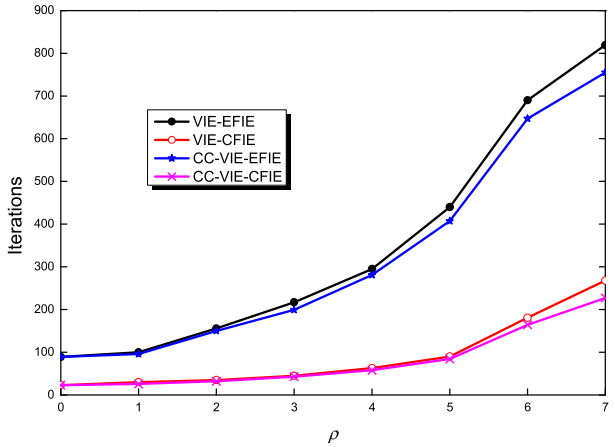

FIGURE 3. Numbers of iterations for four different types of implementations with respect to various ρ as shown in Eq. (35), in the calculation of the coated PEC sphere with inhomogeneous media.

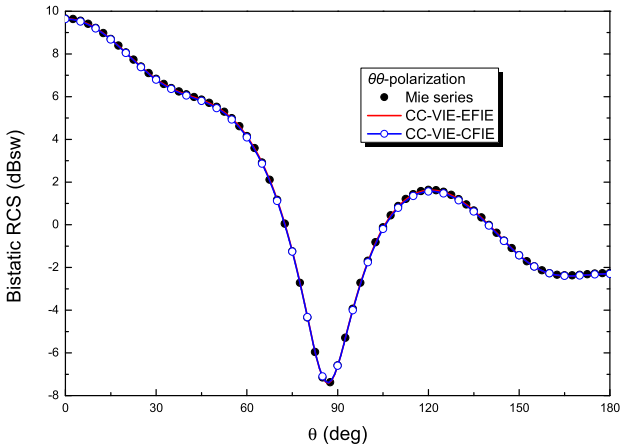

FIGURE 4. Bistatic RCS of co-polarization for a PEC sphere of radius $0.5\lambda_0$, degraded from coated sphere with $\rho = 0$.

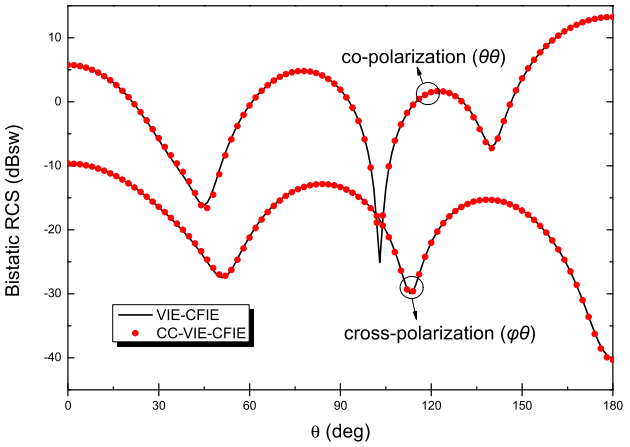

FIGURE 5. Bistatic RCS for a PEC sphere of radius $0.5\lambda_0$ coated with $0.05\lambda_0$ thick extremely inhomogeneous bi-isotropic material with $\rho = 5$.

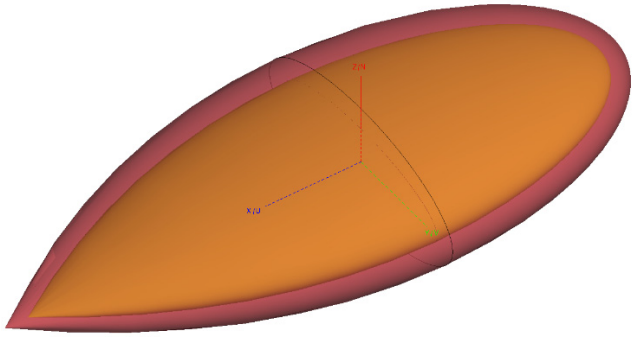

FIGURE 6. The position of the coated PEC almond in the Cartesian coordinates.

It is scarcely possible to simulate this object using the SIE methods. In order to investigate how the medium parameters influence the performances of different implementations, Fig. 3 shows the number of iterations with respect to various ρ. Along with the increase of ρ, the number of iterations will sharply decrease, while the VIE-CFIE always converges several times faster than the VIE-EFIE, particularly when ρ is large. Besides, the use of CC always slightly reduces the number of iterations. When $\rho = 0$ and $\rho = 5$, the numerical results of bistatic RCS from different implementations are shown in Fig. 4 and Fig. 5, respectively, while good agreements are observed. Actually, when $\rho = 0$, the coated material is fictitious, while the "coated" sphere degrades into a PEC sphere. It states that even though the material is extremely inhomogeneous, the use of CC can also keep the accuracy. However, if ρ further increases, due to the coarse average mesh size, the agreement among different implementations will become poor. Table 2 (CS2) lists the computational details with $\rho = 2$.

The third object is a coated PEC almond containing sharp edges and tips [29], whose position in the Cartesian coordinates is shown in Fig. 6. The length of the PEC almond is 9.936 inch, and the coating thickness is 10 mm. The medium parameters of the coated material are $\varepsilon = (3-j2)\varepsilon_0$, $\mu = (2-j)\mu_0, \xi = \zeta* = \upsilon(1-j)\sqrt{\varepsilon_0\mu_0}$, while ξ and $\zeta*$ are the functions of a variable υ. The frequency of incident EM wave is 3 GHz. A moderate mesh size is chosen to generate totally 24,700 unknowns with respect to 1,292 triangles and 4,964 tetrahedrons with $N_{V_2} = 1,292$. The monostatic RCS with different υ is calculated and the observation range is $-90° \leqslant \theta \leqslant 90°$ and $\varphi = 0$, which are shown in Fig. 7. For comparison, the PEC almond without any coated material is also calculated, while the cross-polarization RCS of the PEC almond and the coated almond with $\upsilon = 0$ (in this case, the coated material degrades into isotropy) are below 70 dBsm everywhere, which are not shown. It is observed the effect of the electric and magnetic losses on the reduction of RCS. Besides, under such parameters, with different value of υ, the co-polarization results are almost the same in most angles, while the cross-polarization ones are largely varied. From Fig.6 (b), excellent agreements are observed between the results from VIE-CFIE and those from CC-VIE-CFIE, indicating that when the sharp structures are contained, the use of CC is also valid. The computational details at the direction of $\theta = 90°$ and $\varphi = 0$ are shown in Table 2 (CA).

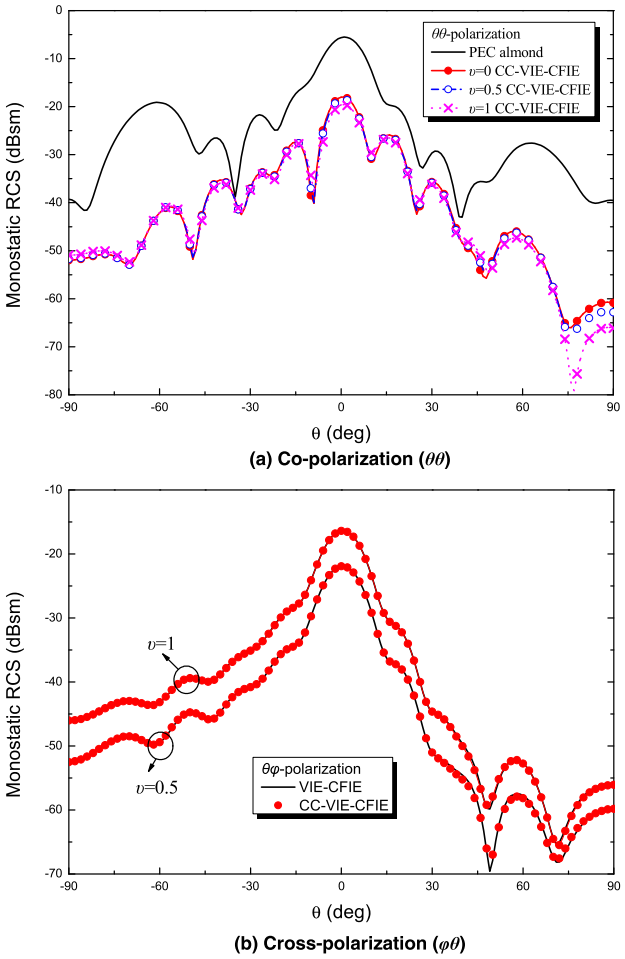

FIGURE 7. Monostatic RCS for a 9.936 inch length PEC almond coated with 10 mm thick inhomogeneous bi-isotropic material with $\varepsilon = (3-j2)\varepsilon_0$, $\mu = (2-j)\mu_0$, $\xi = \zeta* = \upsilon(1-j)\sqrt{\varepsilon_0\mu_0}$ at $-90° \le \theta \le 90°$ and $\varphi = 0$ at 3 GHz.

From the Table 2, it is observed that due to the improvement of matrix condition, the convergence speed of VIE-CFIE is several times faster than that of VIE-EFIE. When the CC is used in either VIE-EFIE or VIE-CFIE, all of the memory usage, the number of iterations, the filling time, and the single iteration time are reduced to some extent. However, for the first coated object CS1, since N_{V_2} occupies a quite small proportion in the total number of unknowns N, this reduction is quite slight. Compared to the method without the CC, the reduction for peak memory usage (*Mem*) using the method with CC is about 6.77%. For the second and the third objects, the reduction of memory requirements and time cost is relatively obvious about 11.1% and 10.7% for peak memory usage (*Mem*), respectively. Therefore, we may draw the conclusion that the CC is more suitable for the calculation of thin-coated objects.

IV. CONCLUSIONS

In the modeling of the EM scattering from the composite objects involving closed PEC surfaces and bi-isotropic materials, the well-conditioned CFIE is used to model the closed PEC surface, which is combined with the VIE to form the VIE-CFIE, a second-kind VSIE form. Compared with the existing articles, the VIE-CFIE scheme is more suitable for the composite closed PEC-bi-isotropic objects. A rigorous MoM solution of the VIE-CFIE has been presented. Based on the commonly used triangular and tetrahedral meshes, the continuity condition (CC) of electric flux is explicitly enforced on the PEC-material interfaces to eliminate the associated volumetric unknowns as well as to reduce the memory usage without compromising the accuracy. The proposed scheme is attractive in analyzing EM problems of thin material coating PEC objects, since the number of unknowns is reduced by a proportion of the total unknowns. Furthermore, the VIE-CFIE enforce CC is convenient to combine with the fast algorithm such as the multilevel fast multipole algorithm (MLFMA) [21]. The efficiency and accuracy of the proposed scheme have been demonstrated by several illustrative numerical examples.

APPENDIX

In this Appendix, we will show how to evaluate the matrix entries in the matrix equation (19). It can be seen that the matrix entries rely on the evaluation of four kinds of integrations as

$$\begin{cases} I_1 = \left\langle \vec{g}_j, \vec{f}_i \right\rangle \\ I_2 = \left\langle \vec{g}_j, \vec{P}_{T_i}\left(\vec{f}_i\right) \right\rangle \\ I_3 = \left\langle \vec{g}_j, \vec{K}_{T_i}\left(\vec{f}_i\right) \right\rangle \\ I_4 = \left\langle \vec{g}_j, \vec{Q}_{T_i}\left(\vec{f}_i\right) \right\rangle \end{cases} \quad \begin{array}{l} \vec{g}_j = \vec{f}_j^{\,S}(\vec{r}), \vec{f}_j^{\,S}(\vec{r}) \times \hat{n}(\vec{r}), \vec{f}_j^{\,V}(\vec{r}) \\ \vec{f}_i = \vec{f}_i^{\,S}, \vec{f}_i^{\,V} \end{array} \tag{36}$$

Apparently, I_1 is nonzero only when the jth testing and ith basis functions have a common domain, which is non-singular everywhere and can be evaluated analytically or numerically. When $\vec{r}$ is far from $\vec{r}'$, I_2, I_3 and I_4 can be easily evaluated using a universal quadrature rule. The inner integration of I_2 has singularity of order one during $\vec{r} \to \vec{r}'$, which can be expediently handled using either singularity extraction method [30] or Duffy transform [31]. For I_3, the inner integration needs to be translated according to

$$\begin{aligned} &\int_{T_i} \left(\vec{r}' - \vec{r}_i\right) \times \nabla G\left(\vec{r}, \vec{r}'\right) dT' \\ &\quad = \int_{T_i} \left[(\vec{r} - \vec{r}_i) + \left(\vec{r}' - \vec{r}\right)\right] \times \nabla G\left(\vec{r}, \vec{r}'\right) dT' \\ &\quad = (\vec{r} - \vec{r}_i) \times \int_{T_i} \nabla G\left(\vec{r}, \vec{r}'\right) dT' \end{aligned} \tag{37}$$

where $\vec{r}_i$ is the free vertex of the ith RWG/SWG basis function. This translation leads to an integration with a singular kernel ∇G that can be numerically handled [30].

I_4 can be rewritten as

$$\begin{aligned} I_4 &= \int_{T_j} \vec{g}_j \cdot \nabla \int_{\tau_i} \nabla' \cdot \vec{f}_i G\left(\vec{r}, \vec{r}'\right) dT' dT \\ &= -\int_{T_j} \nabla \cdot \vec{g}_j \int_{\tau_i} \nabla' \cdot \vec{f}_i G\left(\vec{r}, \vec{r}'\right) dT' dT \\ &\quad + \int_{T_j} \nabla \cdot \left[\vec{g}_j \int_{\tau_i} \nabla' \cdot \vec{f}_i G\left(\vec{r}, \vec{r}'\right) dT'\right] dT \end{aligned} \quad (38)$$

The first term has the singularity of order one during $\vec{r} \to \vec{r}'$, which can be expediently calculated. Especially when $\vec{g}_j = \vec{f}_j^S(\vec{r}) \times \hat{n}(\vec{r})$, since $\nabla \cdot \vec{g}_j \equiv 0$, the first term is equal to 0. According to the Gauss theorem, the second term of I_4 can be transformed as

$$\begin{aligned} &\int_{\tau_j} \nabla \cdot \left[\vec{g}_j \int_{\tau_i} \nabla' \cdot \vec{f}_i G\left(\vec{r}, \vec{r}'\right) dT'\right] dT \\ &= \oint_{\partial T_j} \hat{n}_{\partial T_j} \cdot \left[\vec{g}_j \int_{T_i} \nabla' \cdot \vec{f}_i G\left(\vec{r}, \vec{r}'\right) dT'\right] d(\partial T) \end{aligned} \quad (39)$$

where ∂T_j denotes the three edges bounding the triangle for $T = S$ or the four triangular faces bounding the tetrahedron for $T = V$, while $\hat{n}_{\partial T_j}$ denotes the outward unit normal direction of edges or faces. Then, (39) has singularity of order one during $\vec{r} \to \vec{r}'$, which can be evaluated numerically. Actually, only when $\vec{g}_j$ is a "half" SWG function or $\vec{f}_j^S(\vec{r}) \times \hat{n}(\vec{r})$, does this term need to be evaluated. Otherwise, when $\vec{g}_j$ denotes a RWG or "full" SWG function, due to the property of RWG basis function at ∂S_j or that of SWG function at ∂V_j, the value of (39) is identically equal to 0.

The above expressions (36)-(39) lead to straightforward evaluation of matrix elements of (19).

REFERENCES

[1] A. J. Viitanen and I. V. Lindell, "Chiral slab polarization transformer for aperture antennas," *IEEE Trans. Antennas Propag.*, vol. 46, no. 9, pp. 1395–1397, Sep. 1998.
[2] W. Y. Yin, W. B. Wang, and P. Li, "Guided electromagnetic waves in gyrotropic chirowaveguides," *IEEE Trans. Microw. Theory Techn.*, vol. 42, no. 11, pp. 2156–2163, Nov. 1994.
[3] C. W. Qiu, H. Y. Yao, L. W. Li, S. Zouhdi, and T. S. Yeo, "Backward waves in magnetoelectrically chiral media: Propagation, impedance, and negative refraction," *Phys. Rev. B, Condens. Matter*, vol. 75, Apr. 2007, Art. no. 155120.
[4] V. K. Varadan, V. V. Varadan, and A. Lakhtakia, "On the possibility of designing anti-reflection coatings using chiral composites," *J. Wave-Mater. Interact.*, vol. 2, no. 1, pp. 71–81, 1987.
[5] A. Serdyukov, I. Semchenko, S. Tretyakov, and A. Sihvola, *Electromagnetics of Bi-Anisotropic Materials-Theory and Application*. Amsterdam, The Netherlands: Gordon and Breach, 2001.
[6] I. V. Lindell, A. H. Sihvola, S. A. Tretyakov, and A. J. Viitanen, *Electromagnetic Waves in Chiral and Bi-Isotropic Media*. Norwood, MA, USA: Artech House, 1994.
[7] H. X. Zheng, X. Q. Sheng, and E. K. N. Yung, "Computation of scattering from conducting bodies coated with chiral materials using conformal FDTD," *J. Electromagn. Waves Appl.*, vol. 18, no. 11, pp. 1471–1484, 2004.
[8] Y. J. Zhang and E. P. Li, "Scattering of three-dimensional chiral objects above a perfect conducting plane by hybrid finite element method," *J. Electromagn. Waves Appl.*, vol. 19, no. 11, pp. 1535–1546, 2005.
[9] D. X. Wang, P. Y. Lau, E. K. N. Yung, and R. S. Chen, "Scattering by conducting bodies coated with bi-isotropic materials," *IEEE Trans. Antennas Propag.*, vol. 55, no. 8, pp. 2313–2319, Aug. 2007.
[10] D. X. Wang, E. K. N. Yun, R. S. Chen, and P. Y. Lau, "An efficient volume integral equation solution to EM scattering by complex bodies with inhomogeneous bi-isotropy," *IEEE Trans. Antennas Propag.*, vol. 55, no. 7, pp. 1970–1981, Jul. 2007.
[11] Y. Shi and C. H. Chan, "Solution to electromagnetic scattering by bi-isotropic media using multilevel Green's function interpolation method," *Prog. Electromagn. Res.*, vol. 97, pp. 259–274, 2009.
[12] M. Li, T. Zhuang, and R. S. Chen, "Volume integral equation equivalence principle algorithm domain decomposition with body of revolution equivalence surface," *IET Microw., Antennas Propag.*, vol. 12, no. 3, pp. 375–379, 2018.
[13] M. Li, M. A. Francavilla, R. S. Chen, and G. Vecchi, "Nested equivalent source approximation for the modeling of penetrable bodies," *IEEE Trans. Antennas Propag.*, vol. 65, no. 2, pp. 954–959, Feb. 2017.
[14] X. Li, L. Lei, H. Zhao, L. Guo, M. Jiang, Q. Cai, Z. Nie, and J. Hu, "Efficient solution of scattering from composite planar thin dielectric-conductor objects by volume-surface integral equation and simplified prism vector basis functions," *IEEE Trans. Antennas Propag.*, vol. 66, no. 5, pp. 2686–2690, May 2018.
[15] R. F. Harrington, *Field Computation by Moment Methods*. New York, NY, USA: MacMillan, 1968.
[16] W. C. Chew, J. M. Jin, E. Michielssen, and J. M. Song, *Fast and Efficient Algorithms in Computational Electromagnetics*. Boston, MA, USA: Artech House, 2001.
[17] A. F. Peterson, S. L. Ray, and R. Mittra, *Computational Methods for Electromagnetics*. Piscataway, NJ, USA: IEEE Press, 1998.
[18] C. C. Lu and W. C. Chew, "A coupled surface-volume integral equation approach for the calculation of electromagnetic scattering from composite metallic and material targets," *IEEE Trans. Antennas Propag.*, vol. 48, no. 12, pp. 1866–1868, Dec. 2000.
[19] K. Xiao, S. L. Chai, and L. W. Li, "Comparisons of coupled VSIE and noncoupled VSIE formulations," *J. Wave-Mater. Interact.*, vol. 25, no. 10, pp. 1341–1351, 2011.
[20] O. S. Kim, P. Meincke, O. Breinbjerg, and E. Jørgensen, "Solution of volume-surface integral equations using higher-order hierarchical Legendre basis functions," *Radio Sci.*, vol. 42, no. 4, 2007, Art. no. RS4023.
[21] M. He, J. Liu, B. Wang, C. Zhang, and H. Sun, "On the use of continuity condition in the fast solution of volume-surface integral equation," *IEEE Antennas Wireless Propag. Lett.*, vol. 16, pp. 625–628, Jul. 2017.
[22] E. H. Neuman and M. R. Schrote, "On the current distribution for open surfaces," *IEEE Trans. Antennas Propag.*, vol. AP-31, no. 3, pp. 1550–1553, May 1983.
[23] S. M. Rao, D. R. Wilton, and A. W. Glisson, "Electromagnetic scattering by surfaces of arbitrary shape," *IEEE Trans. Antennas Propag.*, vol. AP-30, no. 3, pp. 409–418, May 1982.
[24] D. H. Schaubert, D. R. Wilton, and A. W. Glisson, "A tetrahedral modeling method for electromagnetic scattering by arbitrarily shaped inhomogeneous dielectric bodies," *IEEE Trans. Antennas Propag.*, vol. AP-32, no. 1, pp. 77–85, Jan. 1984.
[25] Y. Saad, *Iterative Methods for Sparse Linear Systems*, 2nd ed. Philadelphia, PA, USA: SIAM, 2003.
[26] D. A. Dunavant, "High degree efficient symmetrical Gaussian quadrature rules for the triangle," *Int. J. Numer. Methods Eng.*, vol. 21, no. 6, pp. 1129–1148, 1985.
[27] P. Keast, "Moderate-degree tetrahedral quadrature formulas," *Comput. Methods Appl. Mech. Eng.*, vol. 55, no. 3, pp. 339–348, 1986.
[28] L. Gurel and O. Ergul, "Singularity of the magnetic-field integral equation and its extraction," *IEEE Antennas Wireless Propag. Lett.*, vol. 4, no. 1, pp. 229–232, Aug. 2005.
[29] A. C. Woo, H. T. G. Wang, M. J. Schuh, and M. L. Sanders, "EM programmer's notebook-benchmark radar targets for the validation of computational electromagnetics programs," *IEEE Trans. Antennas Propag.*, vol. 35, no. 1, pp. 84–89, Feb. 1993.
[30] D. R. Wilton, S. M. Rao, A. W. Glisson, D. H. Schaubert, O. M. Al-bundak, and C. M. Butler, "Potential integrals for uniform and linear source distributions on polygonal and polyhedral domains," *IEEE Trans. Antennas Propag.*, vol. AP-32, no. 3, pp. 276–281, Mar. 1984.
[31] M. G. Duffy, "Quadrature over a pyramid or cube of integrands with a singularity at a vertex," *SIAM J. Numer. Anal.*, vol. 19, no. 6, pp. 1260–1262, 1982.

JINBO LIU received the B.S. degree in electronic information engineering from Zhengzhou University, Zhengzhou, China, in 2010, and the Ph.D. degree in electronic science and technology from the Beijing Institute of Technology, Beijing, China, in 2016.

He is currently a Lecturer with the School of Information and Communication Engineering, Communication University of China, Beijing. His current research interests include computational electromagnetics, parallel computation, and numerical analysis of antenna array.

ZENGRUI LI received the B.S. degree in communication and information systems from Beijing Jiaotong University, Beijing, China, in 1984, the M.S. degree in electrical engineering from the Beijing Broadcast Institute, Beijing, in 1987, and the Ph.D. degree in electrical engineering from Beijing Jiaotong University, Beijing, in 2009.

He is currently a Professor with the School of Information and Communication Engineering, Communication University of China, Beijing. He has studied at the Yokohama National University, Yokohama, Japan, from 2004 to 2005. His research interests include the areas of finite-difference time-domain (FDTD) methods, electromagnetic scattering, metamaterials, and antennas.

Prof. Li is a Senior Member of the Chinese Institute of Electronics.

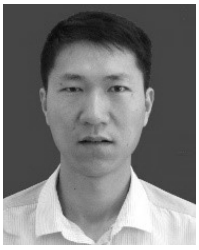

JIANXUN SU received the B.S. degree in electronic information engineering from the Taiyuan University of Technology, Taiyuan, China, in 2006, the M.S. degree from the Communication University of China, in 2008, and the Ph.D. degree in electromagnetic field and microwave technology from the Beijing Institute of Technology, Beijing, China, in 2011.

From 2012 to 2014, he was with the China Electronics Technology Group Corporation (CETC), where he was involved in phased-array system research. He is currently an Associate Researcher with the School of Information and Communication Engineering, Communication University of China. His special research interests include integral equation method, metamaterial, array antenna, and radar target characteristics.

JIMING SONG (S'92–M'95–SM'99–F'14) received the B.S. and M.S. degrees in physics from Nanjing University, China, in 1983 and 1988, respectively, and the Ph.D. degree in electrical engineering from Michigan State University, East Lansing, MI, USA, in 1993.

From 1993 to 2000, he was a Postdoctoral Research Associate, a Research Scientist, and a Visiting Assistant Professor with the University of Illinois at Urbana–Champaign. From 1996 to 2000, he worked part-time as a Research Scientist with SAIC-DEMACO. He was a Principal Staff Engineer/Scientist at Semiconductor Products Sector, Motorola, Tempe, AZ, USA, before joining the Department of Electrical and Computer Engineering, Iowa State University, as an Assistant Professor, in 2002. He was the principal author of the *Fast Illinois Solver Code* (FISC). He is currently a Professor with Iowa State University's Department of Electrical and Computer Engineering, and also a Visiting Professor with the School of Information and Communication Engineering, Communication University of China, Beijing, China. His research has dealt with modeling and simulations of interconnects on lossy silicon and RF components, electromagnetic wave scattering using fast algorithms, the wave propagation in metamaterials, acoustic and elastic wave propagation and non-destructive evaluation, and transient electromagnetic field.

Dr. Song was selected as a National Research Council/Air Force Summer Faculty Fellow, in 2004 and 2005, respectively, and received the NSF Career Award, in 2006. He is an ACES Fellow, and an Associate Editor of the IEEE ANTENNAS AND WIRELESS PROPAGATION LETTERS (AWPL), and ACES Express.